Theoretical Study of the Benzene Dimer by the Density-Functional-Theory Formalism Based on Electron-Density Partitioning

by **Fabien Tran**, **Jacques Weber**, and **Tomasz A. Wesołowski***

Department of Physical Chemistry, University of Geneva, 30, quai Ernest-Ansermet, CH-1211 Geneva 4

Dedicated to Professor *Edgar Heilbronner* on the occasion of his 80th birthday

The density-functional approach based on the partition into subsystems was applied to study the benzene dimer. For several structures, the calculated interaction energy and intermolecular distance were compared with the previous theoretical results. A good agreement with high level *ab initio* correlated methods was found. For instance, the interaction energies obtained in this work and the CCSD(T) method agree within 0.1 – 0.6 kcal/mol depending on the structure of the dimer. The structure with the largest interaction energy is T-shaped, in agreement with CCSD(T) results. The T-shaped structure of benzene dimer was suggested by several experimental measurements. The calculated interaction energy of 2.09 kcal/mol agrees also well with experimental estimates based on the dissociation energy which ranges from 1.6 ± 0.2 to 2.4 ± 0.4 kcal/mol and the estimated zero-point vibration energy of 0.3 – 0.5 kcal/mol.

1. Introduction. – Current implementation of approaches based on density-functional theory (DFT) or *ab initio* methods makes it possible to study relatively large organic systems by means of computer modelling. Such studies might be useful to interpret experimental results by calculating molecular properties such as geometries, dipole moments, electrostatic potentials, reactivity indices, *etc.* [1]. Moreover, the computational methods can be applied to estimate the bonding energies, reaction barriers, and reaction energetics. The computational studies can be used also to determine reaction pathways. The predictive power of such calculations hinges on the accuracy of the theoretical approach used. Although there is a clear hierarchy of *ab initio* theoretical methods that culminates in the so-called chemical accuracy for any molecular system, their practical applications are limited to systems of a rather small size. Most of the interesting problems in organic chemistry lie, therefore, outside of the range of applicability of this accurate theoretical approach. Moreover, experience shows that even moderately accurate theoretical methods can be used as a tool to assist experimental research. Let us take molecular geometry as an example. In DFT, calculations based on local-density approximation (LDA) lead usually to very good geometries for covalently bound complexes. The bond lengths agree within 0.01 – 0.03 Å with experimental measurements. However, the accuracy of the energies calculated by the same approach is not satisfactory (atomization energies differ frequently from experimental values by as much as 10 kcal/mol). It is worthwhile to recall here that LDA is the simplest nonempirical variant of DFT. It is appealing, therefore, to use computer simulations based on approximate methods to study large systems of interest in organic chemistry. Unfortunately, as far as these methods are concerned, a clear hierarchy of approaches leading to exact results does not exist yet in

DFT. To apply an approximate computational method efficiently, its advantages and flaws must be well understood. In this work, we address one very important issue of DFT, namely the weak nonbonding (or *van der Waals*) interactions. Such interactions play a very important role in determining the structure of large flexible molecules (biomolecules, polymers). Weak nonbonding interactions influence significantly the properties of solvated molecules and systems physisorbed on different surfaces. They also determine the steric barriers which might influence reaction pathways.

Since the computational cost of accurate wave-function based methods is prohibitively large for systems of the size of benzene dimer, practical implementations of density-functional theory applicable to the study of weak intermolecular complexes are highly desirable. Unfortunately, applying DFT in its conventional *Kohn-Sham* [2] formulation to study weak complexes faces serious difficulties, because *London* dispersion forces can not be properly accounted for by means of semi-local approximate functionals of exchange-correlation energy. The unsuitability of semi-local functionals may be illustrated by considering the extreme case of two spherically symmetric centers with nonoverlapping electron densities. In such a case, all semi-local exchange-correlation functionals do lead to no attraction between the centers. In real intermolecular complexes, the electron-density overlap is usually small but non-negligible, and different approximate exchange-correlation functionals describe the corresponding energetical components in a rather erratic way [3–7]. The local density approximation leads systematically to too strong attraction, whereas the results of the generalized gradient-approximation (GGA) calculations depend critically on the choice of the applied exchange-correlation functional [8]. Among the GGA functionals, the ones developed recently by *Perdew* and co-workers (PW91 [9], PBE [10]) appear the most suitable for weak complexes leading to rather reasonable interaction energies for complexes in which dispersion forces are known to dominate [5][6][8][11]. But even these functionals lead to less reliable results than correlated wave-function based approaches.

In this work, we explore the applicability of another DFT route to obtain the interaction energies of weak intermolecular complexes which is based on partitioning of total electron density [12][13]. In this approach, the total electron density is partitioned into two subsystems, and the total energy can be minimized with respect to variations of electron density restricted to a selected subsystem. The computer implementation of our subsystems-based approach was recently refined [14–16] and applied to study the properties of embedded molecules [17] as well as different intermolecular complexes including those interacting by H-bonding [16] and weak complexes comprising benzene [18]. The latter studies showed that the subsystems-based approach leads to results usually superior to those obtained using conventional *Kohn-Sham* calculations. Moreover, the results are less dependent on the choice of the approximate functionals than the corresponding *Kohn-Sham* ones.

Here, we apply the subsystems-based approach to the benzene dimer. The method will be described in the next section.

The benzene-benzene interaction is of the nonbonding type, and it is the prototype of π-π interaction between aromatic molecules that influences the structure of such biopolymers as proteins and DNA. The interaction energy of the benzene dimer consists principally of dispersion, electrostatic, and exchange-repulsion energies. The

dispersion energy, which is due to the electronic correlations effects, is always attractive and decreases as R^{-6}, where R is the separation between centers of mass of the two benzene moieties. It is largest for the sandwich structure **e** (*Fig. 1*) and smallest for the T-shaped structures **a**–**d**. The electrostatic energy arises principally from the interaction between permanent quadrupoles of the benzenes and decreases as R^{-5}. Depending on the relative orientation of the benzenes, the electrostatic interaction can be attractive or repulsive; it is attractive for the T-shaped structure and repulsive for the sandwich structure. The exchange-repulsion energy, which is linked to the overlap of occupied orbitals of the two interacting molecules, is repulsive, preventing the two benzenes from approaching too closely. Some experimental [19–39] and theoretical [40–66] results related to the benzene dimer are available in the literature, but the detailed structure is still not known.

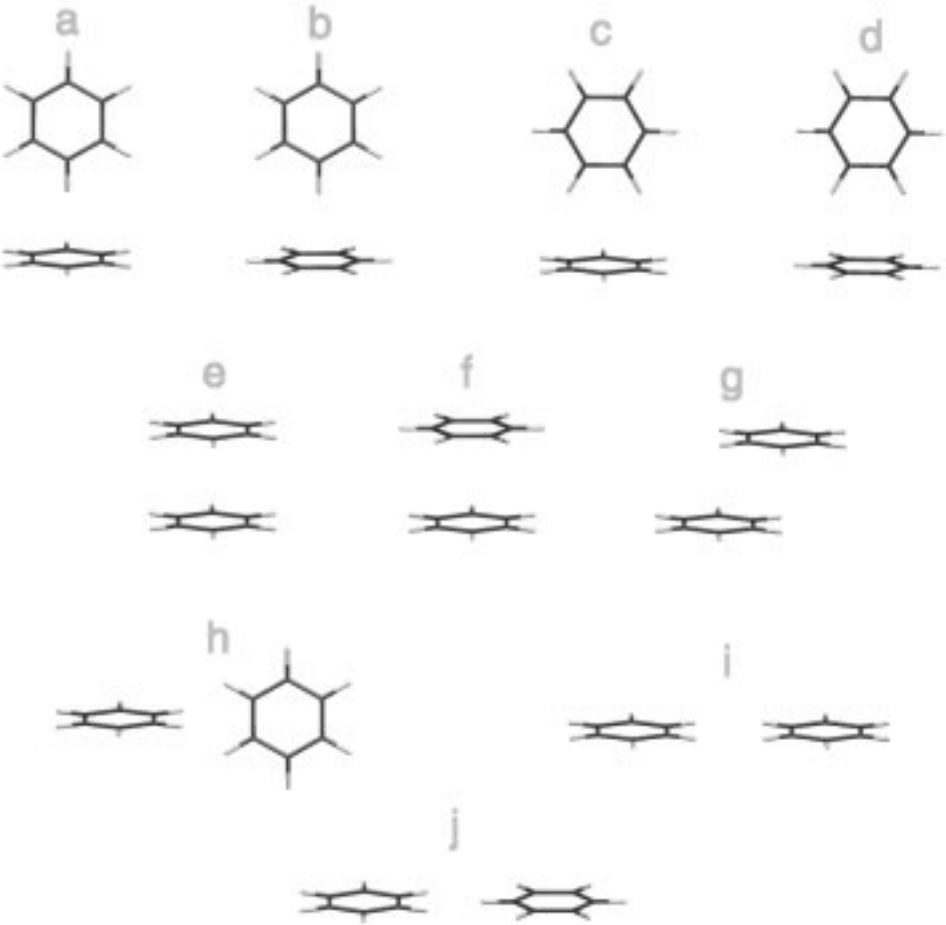

Fig. 1. *Different structures of the benzene dimer studied in this work*

Klemperer and co-workers [20][21] deduced from measurements of the electric deflection of molecular beams that the benzene dimer is polar and an asymmetric top, which could be the T-shaped structure. In solid benzene, neutron-diffraction experiments [19] revealed that the structures correspond to parallel displaced and T-shaped orientations of the benzene molecules, such as the ones observed for the aromatic residues in protein crystal structures [35][36]. Using mass-selected, resonantly enhanced two-color ionization spectroscopy (R2PI), *Hopkins et al.* [22] obtained the $S_1 \leftarrow S_0$ excitation spectrum of the benzene dimer. They found that the 6^1 vibration is split in the dimer by nearly the same amount as that of the benzene solid, and that the 0_0^0 band is induced nearly as strongly in the dimer as it is in the solid.

Measurements of the vibronic spectra of isotopically substituted benzene dimer indicate that the two benzenes are equivalent by symmetry, which excludes the T-shaped structure [24][25][29][42]. *Schlag* and co-workers [24][25] suggested the V-shaped structure (the dihedral angle between the planes of the two benzenes is estimated to lie between 70° and 90°), whereas *Bernstein* and co-workers [29][42] proposed a parallel displaced structure **g**. Other experimental techniques provide, however, a strong indication that the structure of the benzene dimer is T-shaped. *Henson et al.* [30][31] reported ionization-detected stimulated *Raman* spectroscopy (IDSRS) measurements on benzene dimer isotopomers, and they argued that their results provided evidence for a ground state with symmetrically inequivalent benzene moieties, and then proposed a T-shaped structure in which the benzene moiety at the top of the T is free to rotate about its C_6 axis. The same experimental technique led *Ebata et al.* [33] to the conclusion that two isomers coexist; one with a separation between centers of mass of $R = 3.6$ Å and another with $R = 5.0$ Å. From rotationally resolved spectra of microwave experiments, *Arunan* and *Gutowsky* [34] conclude that the benzene dimer is T-shaped with $R = 4.96$ Å. They pointed out, however, that the existence of another state with lower energy was not excluded. With mass-selected hole-burning spectroscopy, *Schlag*'s group [28] found that at least two stable isomers may be found: the T-shaped and probably the parallel displaced structure at very low temperature.

In summary, the reported experimental results indicate that the T-shaped structure is probably a stable minimum, but other such structures with appreciable population are not excluded. Another explanation for the disagreements between the results of different experiments is the possibility of a rapid interconversion between several local minima separated by low barriers.

The thermodynamic parameters of the benzene dimer were reported by several experimentors [27][37][38]: the dissociation energy D_0 was estimated by *Grover et al.* [37] to be 2.4 ± 0.4 kcal/mol, and to be 1.6 ± 0.2 kcal/mol by *Krause et al.* [38], who estimated also the zero-point vibration energy to be 0.5 kcal/mol.

There have been a large number of theoretical studies on the benzene dimer. Some of the first *ab initio* studies of the potential-energy surface of the benzene dimer include configuration interaction (CI) calculations of *Karlström et al.* [41], *Hartree-Fock* (HF) calculations of *Čársky et al.* [47], and second-order *Møller-Plesset* (MP2) calculations of *Hobza et al.* [48]. Due to the relatively small basis sets used in these calculations, the results cannot be considered very reliable. More recently, second- and fourth-order *Møller-Plesset* calculations have been reported by *Hobza et al.* [50][51][53][54], *Jaffe*

et al. [61], and *Tsuzuki et al.* [56–59], the latter authors having performed an extensive study of the basis set truncation error. *Hobza et al.* [53] and *Tsuzuki et al.* [58][59] also carried out calculations with coupled-cluster singles and doubles theory with perturbational triples corrections (CCSD(T)), which are the most accurate *ab initio* results currently available. In the following, these CCSD(T) results will be considered as a reference for comparison. Compared to experimental and highly accurate CCSD(T) results, the MP2 method overestimates the interaction energies, and the most stable structure is the parallel displaced structure (CCSD(T) results are slightly in favour of the T-shaped structure). Due to the large contribution of dispersion interactions, the *Hartree-Fock* theory leads to rather unsatisfactory results for the benzene dimer [47]. Also, the reported DFT calculations based on *Kohn-Sham* equations and applying different exchange-correlation functionals do not lead to satisfactory results [52][59][62].

Using the *Fraga* potentials, *Rubio et al.* [45] have studied different structures of the benzene dimer. They calculated the interaction energy and determined the nature of the stationary points. Other recent studies of the benzene dimer are those of *Chipot et al.* [60], who performed gas-phase simulations with molecular mechanics, and of *Dang* [66], who have constructed a polarizable potential model for benzene with molecular dynamics. So far, the best results seem to have been obtained with the CCSD(T) method, which is also the most computationally expensive method. There have also been some interesting discussions about the possible existence of a $C-H\cdots\pi$ bond for the T-shaped structure [53][54][64].

2. Method. – We start with a short outline of the *Kohn-Sham* method, the most commonly used DFT formalism. This will provide a necessary reference to the subsystems-based approach applied in this work. According to *Hohenberg-Kohn* theorems [67], the ground-state energy of an electronic system (*e.g.*, atom, molecule, and solid) can be expressed as a functional of the electron density ($E=E[\rho]$). In the conventional *Kohn-Sham* formalism, $E[\rho]$ is expressed using the *Kohn-Sham* total-energy functional $E^{KS}[\rho]$ (atomic units are used in all equations)

$$E^{KS}[\rho] = T_s[\rho] + J[\rho] + E_{xc}[\rho] - \sum_A \int \frac{Z_A}{|\mathbf{r}-\mathbf{R}_A|}\,\rho(\mathbf{r})d\mathbf{r}, \tag{1}$$

$$T_s[\rho] = -\frac{1}{2}\sum_{i=1}^{N} \int \psi_i^*(\mathbf{r})\nabla^2\psi_i(\mathbf{r})d\mathbf{r}, \tag{2}$$

$$J[\rho] = \frac{1}{2}\int\int \frac{\rho(\mathbf{r})\rho(\mathbf{r}')}{|\mathbf{r}-\mathbf{r}'|}\,d\mathbf{r}\,d\mathbf{r}', \tag{3}$$

where $T_s[\rho]$ represents the functional of the kinetic energy in the non-interacting electrons reference system, $J[\rho]$ is the classical *Coulomb* repulsion, and $E_{xc}[\rho]$ denotes the exchange-correlation functional, which accounts for the nonclassical many-body effects. The exact form of $E_{xc}[\rho]$ is unknown and hence must be approximated. The last term of *Eqn. 1* represents the electron-nucleus attraction energy, with the index A running through all the nuclei, of charge Z_A at the position $\mathbf{R}_A$, of the system. The variational principle leads to the one-electron self-consistent equations (*Kohn-Sham*)

$$\left(-\frac{1}{2}\nabla^2 + v_{\text{eff}}(\mathbf{r})\right)\psi_i(\mathbf{r}) = \varepsilon_i\psi_i(\mathbf{r}), \tag{4}$$

$$v_{\text{eff}}(\mathbf{r}) = \int \frac{\rho(\mathbf{r}')}{|\mathbf{r}-\mathbf{r}'|}d\mathbf{r}' + \frac{\delta E_{xc}[\rho]}{\delta\rho} - \sum_A \frac{Z_A}{|\mathbf{r}-\mathbf{R}_A|} \tag{5}$$

$$\rho(\mathbf{r}) = \sum_{i=1}^{N} |\psi_i(\mathbf{r})|^2. \tag{6}$$

In the subsystems-based approach (which will be referred to as *Kohn-Sham* equations with Constrained Electron Density, KSCED), the total energy of a system composed of two subsystems (two molecules forming a weak complex for instance) of densities ρ_1 and ρ_2 is represented as the bi-functional $E^{KSCED}[\rho_1, \rho_2]$ of ρ_1 and ρ_2 [12][13][68]

$$\begin{aligned} E^{KSCED}[\rho_1,\rho_2] = E^{KS}[\rho_1+\rho_2] &= T_s[\rho_1] + T_s[\rho_2] + T_s^{nadd}[\rho_1,\rho_2] \\ &+ \frac{1}{2}\int\int \frac{(\rho_1(\mathbf{r})+\rho_2(\mathbf{r}))(\rho_1(\mathbf{r}')+\rho_2(\mathbf{r}'))}{|\mathbf{r}-\mathbf{r}'|}d\mathbf{r}\,d\mathbf{r}' \\ &+ E_{xc}[\rho_1+\rho_2] - \sum_A \int \frac{Z_A}{|\mathbf{r}-\mathbf{R}_A|}(\rho_1(\mathbf{r})+\rho_2(\mathbf{r}))d\mathbf{r}, \end{aligned} \tag{7}$$

where $T_s^{nadd}[\rho_1, \rho_2]$ denotes the nonadditive kinetic energy bi-functional which is defined as

$$T_s^{nadd}[\rho_1,\rho_2] = T_s[\rho_1+\rho_2] - T_s[\rho_1] - T_s[\rho_2]. \tag{8}$$

As in the case of exchange-correlation functional, the analytic form of $T_s^{nadd}[\rho_1, \rho_2]$ is not known, and any practical calculation relies on approximations.

Partitioning of the electron density makes it possible to perform the minimization of the total energy following a step-wise procedure in which the energy is minimized with respect to either ρ_1 or ρ_2 [14]. The electron density ρ_J ($J = 1, 2$) is represented by

$$\rho_J(\mathbf{r}) = \sum_{i=1}^{N_J} |\psi_{i(J)}^{KSCED}(\mathbf{r})|^2, \tag{9}$$

where $\psi_{i(J)}$ is the wave-function of an electron of the subsystem J composed of N_J electrons. Similar steps as those used to derive *Kohn-Sham* equations lead to the following one-electron (KSCED) equations for $\psi_{i(J)}^{KSCED}$ [12][13]:

$$\left(-\frac{1}{2}\nabla^2 + v_{\text{eff}(J)}^{KSCED}(\mathbf{r})\right)\psi_{i(J)}^{KSCED}(\mathbf{r}) = \varepsilon_{i(J)}\psi_{i(J)}^{KSCED}(\mathbf{r}), \tag{10}$$

where

$$\begin{aligned} v_{\text{eff}(J)}^{KSCED}(\mathbf{r}) &= \int \frac{\rho_1(\mathbf{r}')}{|\mathbf{r}-\mathbf{r}'|}d\mathbf{r}' + \int \frac{\rho_2(\mathbf{r}')}{|\mathbf{r}-\mathbf{r}'|}d\mathbf{r}' - \sum_A \frac{Z_A}{|\mathbf{r}-\mathbf{R}_A|} \\ &+ \frac{\delta E_{xc}[\rho_1+\rho_2]}{\delta\rho_J} + \frac{\delta T_s^{nadd}[\rho_1+\rho_2]}{\delta\rho_J} \end{aligned} \tag{11}$$

The use of the KSCED equations to minimize the total energy of the system is performed in several steps (*Fig. 2*). First, the density ρ_1 of subsystem 1 is calculated by means of *Kohn-Sham* equations (cycle 0), then in the next step (cycle 1), the KSCED equations are employed to calculate the density ρ_2 of subsystem 2, which is polarized by subsystem 1. In cycle 2, the role of the two subsystems is interchanged, and the procedure is repeated until convergence, which is often achieved after cycle 2 or even 1.

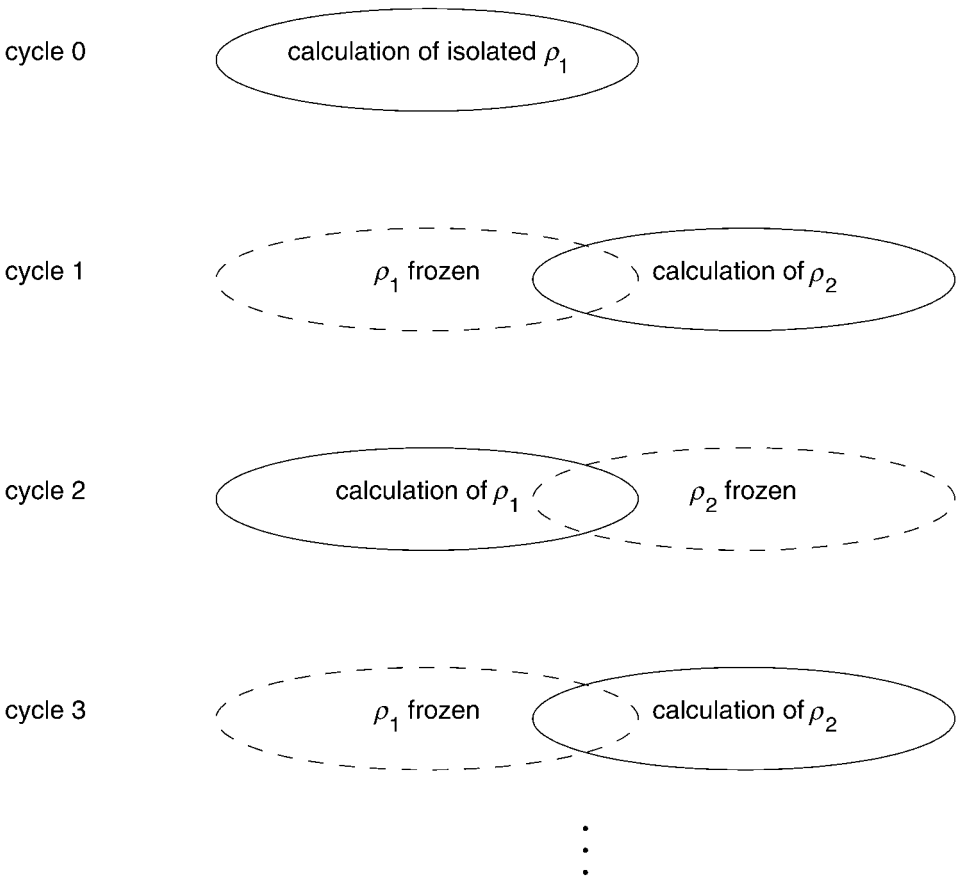

Fig. 2. *Scheme of the 'freeze and thaw' cycle of the KSCED equations*

2.1. *Details of the Calculations.* The calculations were performed with the modified version of the *deMon* program [69] into which the KSCED formalism was implemented [14][69d]. The two subsystems corresponding to electron densities ρ_1 and ρ_2 were identified with the two interacting benzene molecules, respectively, and, during the calculations, the intramolecular geometry of the two benzenes was kept fixed at the experimental geometry [70] ($R_{CC} = 1.397$ Å, $R_{CH} = 1.084$ Å), *i.e.*, only the intermolecular degrees of freedom were varied.

Practical applications of the KSCED scheme rely on the approximations used for $E_{xc}[\rho]$ and $T_s^{nadd}[\rho_1,\rho_2]$. In the current implementation of the KSCED equations, we apply the following approximate functionals:

i) For $E_{xc}[\rho] = E_x[\rho] + E_c[\rho]$, the PW91 functional which has been shown to be the best GGA functional for application to *van der Waals* complexes (see [8] and refs. cit. therein)

$$E_x[\rho] = -C_x \int \rho^{\frac{4}{3}}(\mathbf{r}) F^{\mathrm{PW91}}(s(\mathbf{r}))d\mathbf{r}, \quad E_c[\rho] = E_c^{\mathrm{PW91}}[\rho], \tag{12}$$

where $C_x = (3/4)(3/\pi)^{1/3}$.

ii) For $T_s^{nadd}[\rho_1,\ \rho_2] = T_s[\rho_1+\rho_2] - T_s[\rho_1] - T_s[\rho_2]$, the gradient-dependent functional obtained using the conjecture of *Lee*, *Lee*, and *Parr* [71]

$$T_s[\rho] = C_F \int \rho^{\frac{5}{3}}(\mathbf{r}) F^{\mathrm{PW91}}(s(\mathbf{r}))d\mathbf{r}, \tag{13}$$

where $C_F = (3/10)(3\pi^2)^{2/3}$.

The enhancement factor $F^{\mathrm{PW91}}(s)$ is

$$F^{\mathrm{PW91}}(s) = \frac{1 + 0.19645s\sinh^{-1}(7.7956s) + (0.2743 - 0.1508e^{-100s^2})s^2}{1 + 0.19645s\sinh^{-1}(7.7956s) + 0.004s^4} \tag{14}$$

where $s = |\nabla\rho|/(2\rho k_F)$ is the scaled density gradient with $k_F = (3\pi^2\rho)^{1/3}$ the local *Fermi* vector. It is important to note that the applied approximate functionals of exchange energy and non-additive kinetic energy share the same analytic form of the gradient dependency. The use of the same gradient dependency for the exchange and the kinetic-energy functionals was originally proposed by *Parr* and co-workers [71] who formulated the 'conjointness conjecture', which has been proven and tested for *Hartree-Fock* electron densities [72–74]. Numerical tests have been reported supporting the conjecture also for *Kohn-Sham* electron densities [75]. The use of the same analytic form of the gradient-dependent enhancement factor $F(s)$ in the approximate functionals $E_{xc}[\rho]$ and $T_s^{nadd}[\rho_1,\ \rho_2]$ lies at the origin of the significantly weaker dependence of KSCED results on the particular form of $F(s)$.

The *Kohn-Sham* equations for the calculation of an isolated benzene were performed using the PW91 functional, *Eqn. 12*, for the exchange-correlation energy.

The calculations were carried out using two different orbital basis sets: the first basis (basis I) is Triple Zeta Valence with Polarization (TZVP) [76] with the following contraction pattern (41/11) for H and (7111/411/1*) for C. The second used basis (basis II) was developed by *Partridge* [77][78]. This basis set is labeled in the *deMon* program as O−H MM(7s0p0d) + 4p for H and O−C MM(13s8p0d) + 4d for C. The auxiliary basis sets, with the contraction pattern (5,1) for H and (4,4) for C, were used to fit the electron density [76]. The basis sets are distributed together with the *deMon* package [69]. The exchange-correlation and nonadditive kinetic-energy components of the effective potential were calculated numerically, *i.e.*, without fitting functions. The number of orbital basis functions used for the construction of the electron density ρ_J of the benzene molecule in the complex is the same as that used for the isolated benzene

(the basis functions centered on the atoms of the benzene of interest), and, hence, no basis set superposition error (BSSE) [79] had to be corrected.

3. Results and Discussion. – Ten structures of the benzene dimer were considered (**a**–**j**; *Fig. 1*). For each of these structures, the optimization of geometry has been performed, under the constraints imposed by the symmetry of the structure. The separation between centers of mass R of the two benzenes corresponding to the greatest stability of the structure was found by means of single-point-energy calculations. The interaction energy $\Delta E(R)$ is defined as

$$\Delta E(R) = E_{(C_6H_6)_2}(R) - 2E_{C_6H_6}, \tag{15}$$

where $E_{(C_6H_6)_2}(R)$ is the total energy of the benzene dimer obtained with the KSCED method and $2E_{C_6H_6}$ is the total energy of two infinitely separated benzene molecules (equivalent to the sum of total energies of two isolated benzenes calculated by the *Kohn-Sham* method). Except for structure **g**, the minima on the potential-energy surface were found by means of a one-dimensional scan corresponding to the variation of the intermolecular distance R. For the parallel displaced structure **g**, two degrees of freedom were considered (the distance z between the planes of the two benzenes and the horizontal displacement x).

For each analyzed geometry, to minimize the KSCED total energy bifunctional several 'freeze-and-thaw' cycles were performed (*Fig. 2*). The convergence was generally achieved in the second iteration (cycle 2). *Figs. 3* and *4* show examples of the convergence for the sandwich and parallel displaced structures, **e** and **g**, respectively, for basis I. The KSCED results for the separation between centers of mass R and interaction energy ΔE of the optimized structures are presented in the *Table*, and for comparison, the results obtained with other methods taken from various references are also given.

It may be seen that the choice of basis set does not influence the results significantly, the maximal difference for the intermolecular distance R being 0.05 Å for the structure **h**, and the maximal difference of the calculated interaction energy ΔE being always smaller than 0.1 kcal/mol. In the following, therefore, only the results obtained with basis II will be discussed.

Among the structures studied, the one with the greatest interaction energy ($\Delta E = -2.09$ kcal/mol) is **c** which is T-shaped with $R = 4.80$ Å. The structure **d**, which is less stable than **c** by 0.1 kcal/mol, can be obtained from **c** by rotating one benzene molecule (the lower one of **c** and **d** in *Fig. 1*) by 30° about its C_6 axis. Therefore, we can conclude that in the T-shaped (edge-face) geometry, the rotation of the lower benzene molecule is not free but is slightly hindered because of a barrier of at least 0.1 kcal/mol. The structure **a** is less stable than both the structures **c** and **d** by 0.23 and 0.13 kcal/mol, respectively. This also indicates that the rotation of the upper benzene molecule about its C_6 axis is also hindered. Note that the structures **a** and **c** are related by a 30° rotation. The geometry and thermodynamic parameters of structure **b** are almost identical to those of structure **a**; the position of the minimum is the same and the interaction energy differs by *ca.* 0.01 kcal/mol. This indicates that in this orientation (T-shaped, point-face) the benzenes are free to rotate around the C_6 axis of the lower benzene and hence

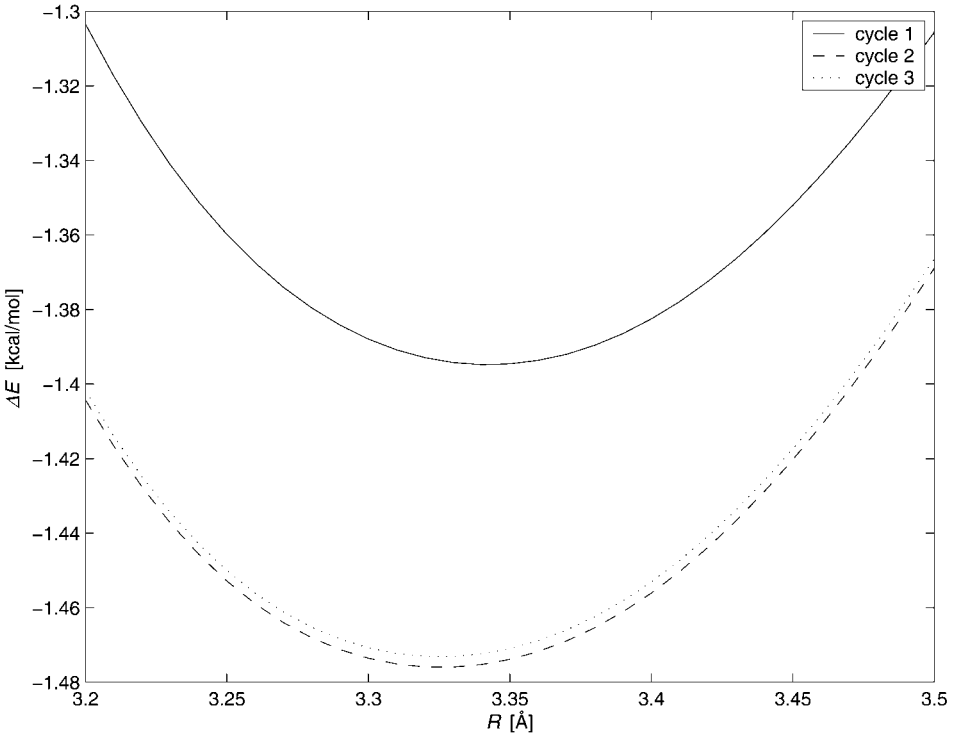

Fig. 3. *Convergence of the potential-energy curve of the sandwich structure* **a** *obtained with basis I*. The separation between centers of mass of the two benzenes is *R*. The curves correspond to different iterations in the 'freeze and thaw' cycle (*Fig. 2*).

constitute an asymmetric top. The sandwich structures **e** and **f**, with their interaction energies amounting to −1.44 and −1.26 kcal/mol, respectively, are less stable than the T-shaped structures. Whereas these smaller interaction energies for the sandwich structures could be explained by the quadrupole-quadrupole electrostatic interaction being attractive for the T-shaped structures, it is of repulsive nature for the sandwich structures and hence destabilizes the dimer in this orientation. For the parallel displaced structure **g**, two minima separated by a small energy barrier of *ca*. 0.05 kcal/mol were found (*Fig. 4* with basis I). For both of them, the distance between the benzene planes (z) equals 3.10 Å, and the horizontal displacement (x) amounts to 2.22 Å for one minimum and 2.95 Å for the other. The interaction energies at these two minima are very close to each other −1.92 and −1.95 kcal/mol, and to the value ΔE for structure **d**. For structure **h**, the interaction energy (−1.62 kcal/mol) is larger than that of sandwich structures. It is smaller, however, than the interaction energy for the T-shaped structures. Finally, the last considered two structures, **i** and **j**, are by far less stable (*ca*. −0.5 kcal/mol).

Turning back to the experimental results, it has been found that for the T-shaped structures **a** and **b** (point-face) the *R* parameter equals 4.96 Å [34], and the lower benzene rotates freely about its C_6 axis [31]. The reported experimental values of the

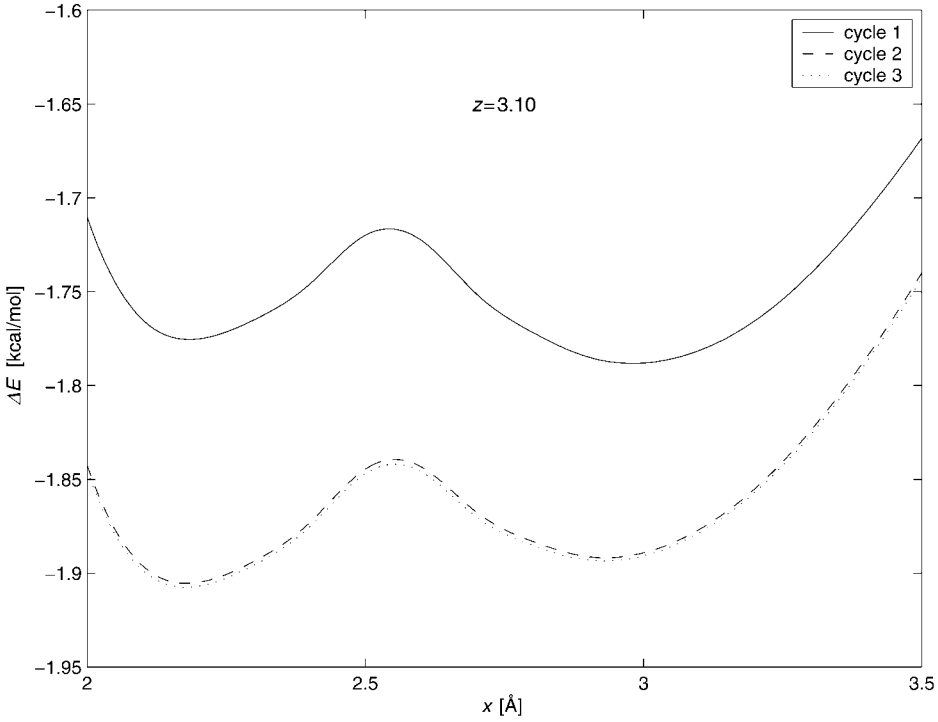

Fig. 4. *Convergence of the potential-energy curve of the parallel displaced structure* **g** *obtained with basis I*. The distance between the planes of the two benzenes is z (3.10 Å), and x is the horizontal displacement. The curves correspond to different iterations in the 'freeze and thaw' cycle (*Fig. 2*).

dissociation energy D_0 (*Table*) fall into a large range (between 1.6 and 2.4 kcal/mol). The zero-point vibration energy was estimated at *ca.* 0.3–0.5 kcal/mol. Combining all the experimental estimates and measurements leads to a rather large range for the depth of the potential minimum D_e, lying roughly between 1.5 and 3 kcal/mol. Since the exact structure of the benzene dimer has not yet been determined experimentally, the above interaction energies can be attributed to one of the possible T-shaped structures and/or perhaps for one or several other isomers. Our KSCED structural results agree well with experimental measurements ($R^{KSCED} = 4.93$ Å, $R^{\exp} = 4.96$ Å). Our calculations indicate, however, that the structures **a** and **b** might not correspond to local minima. The very closely lying structures **c** and **d**, which can be obtained from the structures **a** and **b**, respectively, by rotating the upper benzene around its C_6 axis by 30°, are more stable.

The calculated values of the interaction energy at the lowest points of the potential energy surface considered (−2.09 kcal/mol for structure **c** and *ca.* −1.95 kcal/mol for structures **d** and **g**) fall into the range of the experimental values.

The comparisons of our results with those obtained by other theoretical methods shows that the KSCED and CCSD(T) results agree rather well. For structure **a**, the interaction energies differ by 0.64 kcal/mol, with similar separations between centers of mass. For the sandwich structure **e**, the interaction energies differ by only 0.30 kcal/mol,

Table 1. *KSCED Interaction Energies* ΔE *of the Optimized Structures of the Benzene Dimer Obtained with Basis I and II* (in parenthesis). *R* is the benzene-benzene center of mass separation. Selected results (BSSE-corrected) obtained with other methods, taken from the indicated references are also given.

Structure	Method	R [Å]	$-\Delta E$ [kcal/mol]
a	KSCED	4.94 (4.93)	1.77 (1.86)
	MP2[a])	5.0	3.22
	CCSD(T)[b])	5.0	2.50
	DFT/B3P86[c])	5.6	0.29
	DFT/PW91[d])	5.0	0.65
	Experiment[e])	4.96	
c	KSCED	4.80 (4.80)	2.00 (2.09)
	MP2	5.0[f])	2.51[f])
d	KSCED	4.82 (4.82)	1.91 (1.99)
	DFT/LDA[g])	4.8	2.87
	DFT/BLYP[g])	∞	
e	KSCED	3.33 (3.37)	1.48 (1.44)
	MP2[a])	3.8	3.06
	CCSD(T)[b])	3.8	1.74
	DFT/LDA[g])	3.8	1.20
	DFT/BLYP[c])[g])	∞	
	DFT/B3P86[c])	∞	
f	KSCED	3.40 (3.40)	1.25 (1.26)
g	KSCED	3.80 (3.81)	1.91 (1.92)
		4.27 (4.28)	1.90 (1.95)
	MP2[d])	3.94	4.20
	CCSD(T)[h])	3.85	2.01
	DFT/B3P86[c])	∞	
h	KSCED	5.86 (5.91)	1.62 (1.62)
	MP2[a])	6.22	1.87
i	KSCED	6.78 (6.75)	0.54 (0.56)
j	KSCED	6.63 (6.63)	0.53 (0.53)
	Experiment		$D_0 = 2.4 \pm 0.4$[i])
			$D_0 = 1.6 \pm 0.5$[j])
			$D_0 = 1.6 \pm 0.2$[k])

[a]) From [57]. [b]) From [58]. [c]) From [52]. [d]) From [59]. [e]) From [34]. [f]) From [61]. [g]) From [62]. [h]) From [53]. [i]) From [37]. [j]) From [27]. [k]) From [38].

but the separations between centers of mass differ more ($R = 3.37$ Å for KSCED, $R =$ 3.8 Å for CCSD(T) and MP2). For the parallel displaced structure **g**, the interaction energy obtained with KSCED and CCSD(T) are in remarkable good agreement (-1.95 kcal/mol for KSCED *vs.* -2.01 kcal/mol for CCSD(T)). This agreement must be taken with care because, contrasting with the other geometries discussed so far, the published CCSD(T) results were obtained with medium-quality basis sets for this geometry [53]. The previously discussed CCSD(T) interaction energies for T-shaped and sandwich structures are actually estimations at the basis set limit [58]. For structure **h**, the separation between centers of mass obtained with KSCED is shorter by 0.31 Å than the MP2 one, both methods giving comparable interaction energies (-1.62 kcal/mol for KSCED and -1.87 kcal/mol for MP2).

It is worthwhile to point out that our KSCED results agree better with the high accurate CCSD(T) than the ones of *Møller-Plesset* calculations which systematically overestimate the interaction energies. Compared to *Kohn-Sham* calculations which systematically underestimate the interaction energy (leading sometimes to purely repulsive potential energy curve), the KSCED results are clearly superior.

4. Conclusions. – In this work, the interaction energy of the benzene dimer was calculated by a recently developed DFT approach based on subsystems. As in the previously studied case of other complexes involving benzene [18], good agreement between the calculated and experimental interaction energies is obtained. Our calculations predict that the most stable structure is T-shaped in agreement with experimental results and previously reported benchmark *ab initio* calculations. For several structures, it is shown that the KSCED results follow closely the tendencies found with CCSD(T) calculations. Compared to *Møller-Plesset* calculations and DFT calculations based on *Kohn-Sham* equations, the KSCED method appears superior. This indicates that the KSCED formalism offers a theoretical route to overcome the well-known difficulties of DFT within *Kohn-Sham* framework for weakly bound complexes.

Financial support by the *Federal Office for Education and Science*, acting as *Swiss COST* office, is greatly acknowledged. This work is also part of the Project 21-63645.00 of the *Swiss National Science Foundation*. *T. W.* acknowledges the computer equipment grants from *Fonds Frédéric Firmenich et Philippe Chuit* and *Fondation Ernst et Lucie Schmidheiny*.

REFERENCES

[1] W. Kohn, A. D. Becke, R. G. Parr, *J. Phys. Chem.* **1996**, *100*, 12974.
[2] W. Kohn, L. J. Sham, *Phys. Rev. A* **1965**, *140*, 1133.
[3] S. Kristyán, P. Pulay, *Chem. Phys. Lett*. **1994**, *229*, 175.
[4] J. M. Pérez-Jordá, A. D. Becke, *Chem. Phys. Lett*. **1995**, *233*, 134.
[5] T. A. Wesołowski, O. Parisel, Y. Ellinger, J. Weber, *J. Phys. Chem. A* **1997**, *101*, 7818.
[6] Y. Zhang, W. Pan, W. Yang, *J. Chem. Phys.* **1997**, *107*, 7921.
[7] A. Milet, T. Korona, R. Moszynski, E. Kochanski, *J. Chem. Phys.* **1999**, *111*, 7727.
[8] T. A. Wesołowski, *J. Chem. Phys.* **2000**, *113*, 1666.
[9] J. P. Perdew, J. A. Chevary, S. H. Vosko, K. A. Jackson, M. R. Pederson, D. J. Singh, C. Fiolhais, *Phys. Rev. B* **1992**, *46*, 6671.
[10] J. P. Perdew, K. Burke, M. Ernzerhof, *Phys. Rev. Lett*. **1996**, *77*, 3865; J. P. Perdew, K. Burke, M. Ernzerhof, *Phys. Rev. Lett*. **1997**, *78*, 1396.
[11] D. C. Patton, D. V. Porezag, M. R. Pederson, *Phys. Rev. B* **1997**, *55*, 7454.
[12] P. Cortona, *Phys. Rev. B* **1991**, *44*, 8454.
[13] T. A. Wesołowski, A. Warshel, *J. Phys. Chem*. **1994**, *98*, 5183.
[14] T. A. Wesołowski, J. Weber, *Chem. Phys. Lett*. **1996**, *248*, 71.
[15] T. A. Wesołowski, H. Chermette, J. Weber, *J. Chem. Phys.* **1996**, *105*, 9182.
[16] T. A. Wesołowski, *J. Chem. Phys.* **1997**, *106*, 8516.
[17] T. A. Wesołowski, *Chem. Phys. Lett*. **1999**, *311*, 87.
[18] T. A. Wesołowski, Y. Ellinger, J. Weber, *J. Chem. Phys*. **1998**, *108*, 6078.
[19] E. G. Cox, D. W. J. Cruickshank, J. A. S. Smith, *Proc. R. Soc. London*, *Ser. A* **1958**, *247*, 1.
[20] K. C. Janda, J. C. Hemminger, J. S. Winn, S. E. Novick, S. J. Harris, W. Klemperer, *J. Chem. Phys.* **1975**, *63*, 1419.
[21] J. M. Steed, T. A. Dixon, W. Klemperer, *J. Chem. Phys.* **1979**, *70*, 4940.
[22] J. B. Hopkins, D. E. Powers, R. E. Smalley, *J. Phys. Chem*. **1981**, *85*, 3739.
[23] I. Nishiyama, I. Hanazaki, *Chem. Phys. Lett*. **1985**, *117*, 99.

[24] K. H. Fung, H. L. Selzle, E. W. Schlag, *J. Phys. Chem*. **1983**, *87*, 5113.
[25] K. O. Börnsen, H. L. Selzle, E. W. Schlag, *Z. Naturforsch. A* **1984**, *39*, 1255.
[26] K. O. Börnsen, H. L. Selzle, E. W. Schlag, *J. Chem. Phys*. **1986**, *85*, 1726.
[27] A. Kiermeier, B. Ernstberger, H. J. Neusser, E. W. Schlag, *J. Phys. Chem*. **1988**, *92*, 3785.
[28] W. Scherzer, O. Krätzschmar, H. L. Selzle, E. W. Schlag, *Z. Naturforsch. A* **1992**, *47*, 1248.
[29] K. S. Law, M. Schauer, E. R. Bernstein, *J. Chem. Phys.* **1984**, *81*, 4871.
[30] B. F. Henson, G. V. Hartland, V. A. Venturo, R. A. Hertz, P. M. Felker, *Chem. Phys. Lett*. **1991**, *176*, 91.
[31] B. F. Henson, G. V. Hartland, V. A. Venturo, P. M. Felker, *J. Chem. Phys.* **1992**, *97*, 2189.
[32] V. A. Venturo, P. M. Felker, *J. Chem. Phys.* **1993**, *99*, 748.
[33] T. Ebata, M. Hamakado, S. Moriyama, Y. Morioka, M. Ito, *Chem. Phys. Lett*. **1992**, *199*, 33.
[34] E. Arunan, H. S. Gutowsky, *J. Chem. Phys.* **1993**, *98*, 4294.
[35] C. A. Hunter, J. K. M. Sanders, *J. Am. Chem. Soc*. **1990**, *112*, 5525.
[36] C. A. Hunter, J. Singh, J. M. Thornton, *J. Mol. Biol*. **1991**, *218*, 837.
[37] J. R. Grover, E. A. Walters, E. T. Hui, *J. Phys. Chem*. **1987**, *91*, 3233.
[38] H. Krause, B. Ernstberger, H. J. Neusser, *Chem. Phys. Lett*. **1991**, *184*, 411.
[39] T. Hirata, H. Ikeda, H. Saigusa, *J. Phys. Chem. A* **1999**, *103*, 1014.
[40] D. E. Williams, *Acta Crystallogr.*, *Sect. A* **1980**, *36*, 715.
[41] G. Karlström, P. Linse, A. Wallqvist, B. Jönsson, *J. Am. Chem. Soc*. **1983**, *105*, 3777.
[42] M. Schauer, E. R. Bernstein, *J. Chem. Phys.* **1985**, *82*, 3722.
[43] B. W. van de Waal, *Chem. Phys. Lett*. **1986**, *123*, 69.
[44] F. Torrens, J. Sánchez-Marín, E. Ortí, I. Nebot-Gil, *J. Chem. Soc.*, *Perkin Trans.* **1987**, *2*, 943.
[45] M. Rubio, F. Torrens, J. Sánchez-Marín, *J. Comput. Chem*. **1993**, *14*, 647.
[46] W. L. Jorgensen, D. L. Severance, *J. Am. Chem. Soc*. **1990**, *112*, 4768.
[47] P. Čársky, H. L. Selzle, E. W. Schlag, *Chem. Phys.* **1988**, *125*, 165.
[48] P. Hobza, H. L. Selzle, E. W. Schlag, *J. Chem. Phys.* **1990**, *93*, 5893.
[49] P. Hobza, H. L. Selzle, E. W. Schlag, *J. Phys. Chem*. **1993**, *97*, 3937.
[50] P. Hobza, H. L. Selzle, E. W. Schlag, *J. Am. Chem. Soc*. **1994**, *116*, 3500.
[51] P. Hobza, H. L. Selzle, E. W. Schlag, *Chem. Rev*. **1994**, *94*, 1767.
[52] P. Hobza, J. Šponer, T. Reschel, *J. Comput. Chem*. **1995**, *16*, 1315.
[53] P. Hobza, H. L. Selzle, E. W. Schlag, *J. Phys. Chem*. **1996**, *100*, 18790.
[54] P. Hobza, V. Špirko, H. L. Selzle, E. W. Schlag, *J. Phys. Chem. A* **1998**, *102*, 2501.
[55] V. Špirko, O. Engkvist, P. Soldán, H. L. Selzle, E. W. Schlag, P. Hobza, *J. Chem. Phys.* **1999**, *111*, 572.
[56] S. Tsuzuki, T. Uchimaru, K. Tanabe, *J. Mol. Struct. (Theochem)* **1994**, *307*, 107.
[57] S. Tsuzuki, T. Uchimaru, M. Mikami, K. Tanabe, *Chem. Phys. Lett*. **1996**, *252*, 206.
[58] S. Tsuzuki, T. Uchimaru, K. Matsumura, M. Mikami, K. Tanabe, *Chem. Phys. Lett*. **2000**, *319*, 547.
[59] S. Tsuzuki, H. P. Lüthi, *J. Chem. Phys.* **2001**, *114*, 3949.
[60] C. Chipot, R. L. Jaffe, B. Maigret, D. A. Pearlman, P. A. Kollman, *J. Am. Chem. Soc*. **1996**, *118*, 11217.
[61] R. L. Jaffe, G. D. Smith, *J. Chem. Phys.* **1996**, *105*, 2780.
[62] E. J. Meijer, M. Sprik, *J. Chem. Phys.* **1996**, *105*, 8684.
[63] B. Hernández, F. J. Luque, M. Orozco, *J. Comput. Chem*. **1999**, *20*, 937.
[64] J. J. Novoa, F. Mota, *Chem. Phys. Lett*. **2000**, *318*, 345.
[65] S. Lorenzo, G. R. Lewis, I. Dance, *New J. Chem*. **2000**, *24*, 295.
[66] L. X. Dang, *J. Chem. Phys.* **2000**, *113*, 266.
[67] P. Hohenberg, W. Kohn, *Phys. Rev. B* **1964**, *136*, 864.
[68] R. F. Nalewajski, *Int. J. Quantum Chem*. **2000**, *76*, 252.
[69] a) A. St-Amant, D. R. Salahub, *Chem. Phys. Lett*. **1990**, *169*, 387; b) A. St-Amant, Ph.D. Thesis, University of Montreal **1992**; c) deMon-KS, Version 3.5, M. E. Casida, C. Daul, A. Goursot, A. Koester, L. G. M. Pettersson, E. Proynov, A. St-Amant, and D. R. Salahub principal authors, S. Chretien, H. Duarte, N. Godbout, J. Guan, C. Jamorski, M. Leboeuf, V. Malkin, O. Malkina, M. Nyberg, L. Pedocchi, F. Sim, and A. Vela contributing authors, *deMon Software*, 1998; d) Implementation of KSCED formalism by T. A. Wesołowski in deMon program; T. A. Wesołowski, J. Weber, *Chem. Phys. Lett*. **1996**, *248*, 71.
[70] W. R. Wiley Environmental Molecular Sciences Laboratory, http://www.emsl.pnl.gov:2080/.
[71] H. Lee, C. Lee, R. G. Parr, *Phys. Rev. A* **1991**, *44*, 768.
[72] N. H. March, R. Santamaria, *Int. J. Quantum Chem.* **1991**, *39*, 585.
[73] D. J. Lacks, R. G. Gordon, *J. Chem. Phys.* **1994**, *100*, 4446.
[74] P. Fuentealba, O. Reyes, *Chem. Phys. Lett*. **1995**, *232*, 31.

[75] A. Lembarki, H. Chermette, *Phys. Rev. A* **1994**, *50*, 5328.
[76] N. Godbout, D. R. Salahub, J. Andzelm, E. Wimmer, *Can. J. Chem*. **1992**, *70*, 560.
[77] H. Partridge, *J. Chem. Phys.* **1987**, *87*, 6643.
[78] H. Partridge, *J. Chem. Phys.* **1989**, *90*, 1043.
[79] S. F. Boys, F. Bernardi, *Mol. Phys.* **1970**, *19*, 553.

Received April 2, 2001